

EXPERIMENTAL VALIDATION OF A 2.5D FEM-BEM MODEL FOR THE ASSESSMENT OF VIBRATIONS INDUCED BY TRAFFIC

Alves Costa, P.¹, Calçada, R.², and Silva Cardoso, A.³

^{1,2,3} University of Porto, Faculty of Engineering

R. Dr. Roberto Frias, Porto, Portugal

pacosta@fe.up.pt¹; ruiabc@fe.up.pt²; scardoso@fe.up.pt³

Keywords: Track-ground vibrations induced by railway traffic; numerical modeling; experimental validation

Abstract. This paper presents two main parts, encompassing the experimental assessment and the numerical modelling of vibrations induced by railway traffic. Firstly, a global description of an experimental trial field developed in the Portuguese railway network is presented. In that trial field several tests were performed in order to obtain a reasonable mechanical characterization of the main elements involved in the process of generation and propagation of waves induced by traffic. So as to reach the proposed goal, a geotechnical characterization campaign was performed, including cross-hole tests and specific tests to estimate the ground damping properties. Concerning the track properties, receptance tests and a campaign of measurement of irregularities were conducted. After the global characterization of the site and of the track, vibrations induced by the railway traffic were then measured both in the railway track and in the free-field.

The results of the tests are used in the validation of a 2.5D FEM/BEM model developed by the authors. The model fully accounts for the dynamic interaction between the train, the track and the layered ground. The railway track and embankment, assumed to be invariant in the longitudinal direction, are modelled with 2.5D finite elements [1]. On the other hand, the layered ground below the embankment is simulated by a 2.5D boundary elements formulation. This formulation allows an efficient solution of the track-ground dynamic interaction problem in the frequency-wavenumber domain, as recently explained by François et al. [2]. Regarding the modelling of the rolling stock, a multi-body model is adopted, where the main masses and suspensions of the train are incorporated.

The study, involving experimental and numerical techniques, revealed to be very useful, allowing not only the experimental validation of the numerical model proposed by the authors, but also a deep understanding of the influence of several aspects who determine the problem's solution.

1 INTRODUCTION

The railway is one the most efficient transport systems. Nowadays, it is well known that for middle distances, i.e., lower than 500 km, the energetic efficiency and the comfort associated to the rail transportation turns this transportation system very competitive when compared with the air traffic or with the road transit [3]. However, the sustainable development of modern railway networks should take into account several aspects, few of them neglected in the past.

One particular and important concern is related with the environmental impact that the railway traffic can present on the facilities near to the track, mainly in urban environment, comprising the noise and vibration induced by the train passage. Apart from other issues, the railway traffic can cause discomfort to inhabitants or affect the regular use of sensitive equipments in surrounding buildings. Although structural damage in building is not commonly related to traffic, it is not so unusual the occurrence of some cosmetic damages, which are also unacceptable in the case of important and historical heritage. Therefore, the prediction and assessment of train induced ground vibration is becoming increasingly important, and much attention has been given to this challenge during the last decade, since proposals of empirical prediction models to advanced numerical models. As result, several numerical and semi-analytical models have been proposed. The semi-analytical approaches present a clear supremacy in terms of computation efficiency and capability to the understanding of the phenomena. Many research studies about this subject were carried out since the introduction of the pioneer concept of equivalent stiffness of the ground by Dieterman and Metrikine [3, 4]. An efficient and comprehensive three dimensional model that takes into account the fully interaction train-track-ground was presented by Sheng et al [5]. Despite of the effort dedicated by many researchers in order to improve the semi-analytical models for the incorporation of more complex geometries, the strictness generally found on these solutions does not allow the consideration of the complex geometries usually found in practical applications [6].

The above mentioned limitations, intrinsic to the semi-analytical approaches, combined with the development of computational capabilities, has led to the development of numerical approaches specially designed for the simulation of large domains subjected to moving loads. An efficient approach to the modeling of the dynamic track-ground response can be reached taking advantage of some properties commonly assumed, namely: the linearity and the invariability of the domain along the track direction [7]. These properties allow solving the 3D problem by an efficient computational scheme, usually called 2.5D, which only requires the cross section discretization since the spatial coordinate along the track development is subjected to a domain transformation by a Fourier transform. This procedure is becoming very popular, and several researchers have applied this concept to the formulation of models based on the finite elements approach, and more recently also to the boundary elements approach [1, 8-12]. Recently, François et al [2] presented an efficient and comprehensive approach for coupling between both methods, which was also applied in a study performed by Galvín et al. [13].

Apart from the matters related with the modeling of track-ground response, a lack of experimental validation of proposed models remains. In fact, the number of case studies reported in the bibliography remains very scarce, contributing to the difficulty generally found on the experimental validation of the numerical models.

The aim of this paper is twofold. The first objective is to present a numerical model for the assessment of track-ground vibrations induced by railway traffic. This model was developed by the authors and implemented on the numerical platform Matlab 2009, taking advantage of this platform for the use of parallel computation schemes.

The second objective is to present a set of experiments, developed on a site of the Portuguese railway network, which are used for the validation of this particular numerical model, but can also be used for the validation of further models proposed by other authors.

2 NUMERICAL MODEL

2.1 Generalities

The proposed numerical model is divided into two main modulus: the former includes the track-ground structure, modeled by a 2.5D approach where the tridimensionality of the domain is taken into account: the latter concerns to the simulation of the dynamic of the structural behavior of the train, which is simulated by a multi-body formulation taking into account the main masses and suspensions of the vehicles.

Both formulations are integrated by a compliance formulation in order to take into account the train-track interaction. In following sections the main aspects and assumptions of both methods are described.

2.2 Track-ground simulation by 2.5D FEM-BEM

The track-ground dynamic response induced by train passage is computed by a numerical procedure based on the coupling between finite elements and boundary elements methods, both formulated in the 2.5D domain. Since it is assumed that the dynamic problem is linear, the formulation can be developed in the wavenumber-frequency domain, employing Fourier expansions for space (only in the track development direction) and time. This procedure, called 2.5D, allows obtaining the 3D solutions without the need of numerical discretization along the development direction of the track. A similar model was recently presented by François et al. [2] and Galvín et al. [13].

Domain decomposition is used to solve the dynamic problem, being the track modeled by the 2.5D FEM and the layered ground simulated through 2.5D BEM, as shown in Figure 1.

The coupling between both domains is done by a finite elements formulation, comprising the transformation of the flexibility matrix that governs the dynamic behavior of the BEM domain into a dynamic stiffness matrix.

Following the inner formalism of the 2.5D FEM, the dynamic equilibrium equations of the medium can be reached by the formulation in the variation form. So, for a conservative system, the sum of the virtual work of the internal forces and of the inertial forces is equal to the virtual work of the external forces. After introducing the discretization of the cross-section into 2.5D finite elements and applying a Fourier transform regarding the x coordinate, the dynamic equilibrium can be described by the following system of equations:

$$(K_1^{\text{global}} + ik_1 K_2^{\text{global}} + k_1^2 K_3^{\text{global}} + k_1^4 K_4^{\text{global}} - \omega^2 M^{\text{global}} + K_5^{\text{global}}(k_1, \omega)) \tilde{u}_n(k_1, \omega) = \tilde{p}_n(k_1, \omega) \quad (1)$$

where K_1^{global} to K_4^{global} are stiffness matrices of the domain described by finite elements, M^{global} is the mass matrix, k_1 is the Fourier image of the coordinate x, ω is the frequency, u_n is the vector of the nodal displacements, p_n is the vector of the external forces, and, finally K_5^{global} is the matrix that collects the impedance terms of the layered ground.

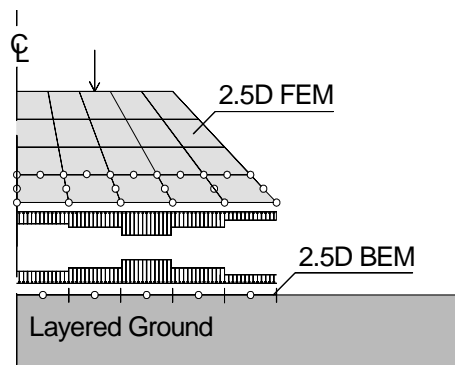


Figure 1 - 2.5D FEM-BEM coupling.

The continuous medium, i.e., the embankment and the granular layers of the track are simulated by 8 nodes finite elements, with exception of the elements that establish the connection between the FEM domain with the BEM domain. In the latter, 7 nodes elements are adopted in order to have two nodes along the side of connection FEM-BEM. Regarding to particular elements of the track, as for instance the sleepers and the rails, a comprehensive description of the modeling strategy can be found on Alves Costa et al. [1]

Since the 2.5D FEM is well explained in several technical documents, including in one paper previously presented by the authors, the deduction of the above mentioned matrices is not presented here again; the reader is advised to consult the following references: [1, 2, 13]. In following, the attention is focalized on the coupling between 2.5 FEM-BEM, which is described by the matrix K_5 .

Several 2.5D boundary integral equations have been proposed during the recent years. Sheng et al. [14] have proposed a 2.5D boundary integral equation based on the reciprocity theorem. More recently, François et al. [2] proposed a new approach based on a regularized version of the boundary integral equation in order to avoid the analytical integration of singular terms. However, the version here presented is simpler, since it is assumed that the coupling between the FEM and BEM domains occurs along the ground surface, not being allowed the embedment of the finite element mesh in the BEM domain. In that case, taking into account the reciprocity theorem and the Somigliana identity, the boundary integral equation assumes the following aspect:

$$u_j(\mathbf{x}, \omega) = \int_{\Sigma} u_{ji}^G(\mathbf{x}, \mathbf{y}, \omega) p_i(\mathbf{y}, \omega) d\Sigma \quad (2)$$

where u_j corresponds to the displacement of the point with coordinates x when a pressure, p_i , is applied along the surface Σ (belonging to the ground surface). On the other hand u_{ji}^G is the tensor of the Green's functions of the displacements.

For the computation of the displacement Green's function several methodologies can be followed. Since the objective is to find the BEM matrices in the 2.5D domain, it looks be natural and, apparently more efficient, the option by the 2.5D Green's function proposed by Tadeu and António [15] for a halfspace instead of other methodology. However, in order to avoid the discretization of the interface between distinct layers, in the present study 3D Green's functions are adopted, which are computed in the transformed domain by resource to a hybrid formulation of Thin-layer method, as proposed by Kausel [16].

The introduction of the ground surface discretization is anteceded by some simplifications that must be mentioned and clarified. In approach followed in the present work, only linear boundary elements are used, with one point of collocation (in the middle of the element) and its dimension is defined by the side length of the neighbor finite element. It should be remem-

bered that the neighbor finite element only presents two nodes along the side of connection FEM-BEM, which means that some error of approximation is allowed between the displacements computed by both methods along the connection surface.

In sum, considering the 2.5D discretization and the schematic representation presented in Figure 2, the BEM equilibrium equation can be described by:

$$u_n(k_1, y_1, 0, \omega) = [G(k_1, y_j - y_i, z_1, \omega)] p_n(k_1, \omega) \quad (3)$$

where u_n is the vector of that collects the displacements of the collocation points; p_n is the vector of the applied pressures along each boundary element and, finally the matrix G corresponds to the flexibility matrix of the domain.

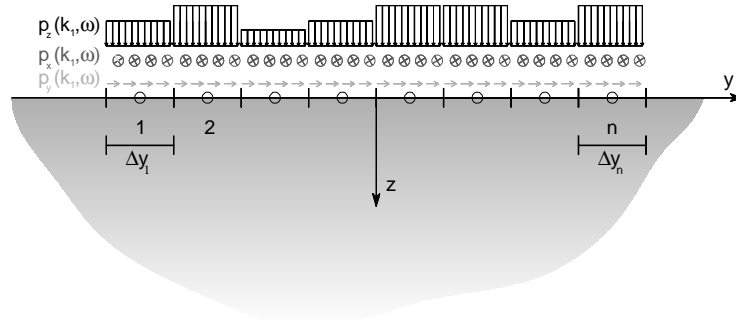


Figure 2- 2.5D ground surface discretization.

The FEM-BEM coupling can be performed by several approaches. In the present study the coupling is done in FEM sense, being the flexibility matrix G transformed into the dynamic stiffness K_5 , through the following relationship:

$$K_5 = [T_q][G(k_1, \omega)]^{-1}[T] \quad (4)$$

where T is a matrix that relates nodal displacements with the homologous evaluated in the collocation points and, T_q is a matrix resulting from the integration of the shape functions (of the finite elements) along the coupling boundary.

Since the motion and equilibrium of the domain is formulated by a 2.5D approach, where Fourier transform are applied over the x coordinate and time, the simulation of moving loads is easy, and can be found in several paper related with this matter .

Solving the equations system presented in (1), the nodal displacements in the transformed domain are obtained, as well as the traction along the coupling boundary. Once these tractions and the Green's functions of the displacements are known, the computation of the free field response is trivial.

2.3 Track-Train interaction

The load applied by the train on the track can be divided into two components: i) the static load, resulting from the weight of the train; ii) the dynamic load, due to the dynamic interaction between the train and the track. As the first component is an input data and not an unknown variable, its consideration on a numerical model is trivial. Unfortunately, the same statement cannot be extended for the latter component, which demands for the solution of the dynamic train-track interaction problem. In the present study, this problem is solved by a compliance procedure formulated in a referential that moves with the train, as suggested by several authors [10, 11, 17, 18].

Assuming perfect contact between both structures, the following relationship must be adhered to at any temporal instant for all connection points between the train and the track:

$$u_{c,i} = u_r(x = ct + a_i) + \Delta u \left(t + \frac{a_i}{c} \right) \quad (5)$$

where u_c represents the vector of vertical displacements of the vehicle in the connection points, u_r is the vector of vertical displacements of the track at the same location; Δu is the rail unevenness; t is the time; a_i is the location of contact point i at $t=0$ s and c is the vehicle speed.

Since the wheelsets are simulated by rigid bodies, the displacement of any axle is equal to the sum of the displacement of the corresponding connection point with the deformation of the Hertzian spring introduced in order to take into account the contact deformation:

$$u_{c,i} = u_r(x = ct + a_i) + \Delta u \left(t + \frac{a_i}{c} \right) + \frac{P_i(t)}{k_H} \quad (6)$$

where k_H is the Hertzian stiffness and P_i is the dynamic interaction force developed at the connection point i .

Equation 5 can be written in matrix form in the frequency domain using the transformation of the unevenness for that domain. So, the train-track interaction force in the frequency domain is given by:

$$P(\Omega) = -([F] + [F]^H + [A])^{-1} \Delta u(\Omega) \quad (7)$$

where $[F]$ is the train compliance at the contact points with the track, $[F]^H$ is a diagonal matrix where the terms are equal to $1/k_H$ and $[A]$ is the compliance matrix of the track. All matrices are square with a dimension equivalent to the number of wheelsets and its deduction can be found in Alves Costa et al. [19]

Analyzing equation 7, one can conclude that the influence of the vehicle properties and of the modeling strategy used only affects matrix $[F]$. A simple but general vehicle model, which takes into account the main structural aspects of the train dynamics, was proposed by Zhai e Cai [20] (Figure 3).

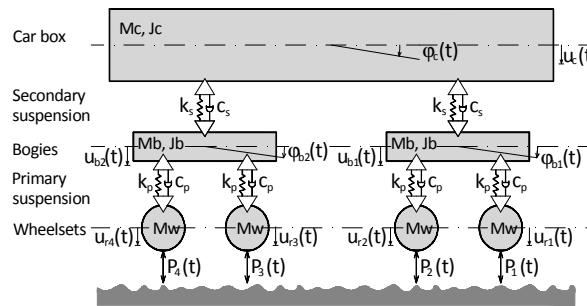


Figure 3 - Complete 2D vehicle model.

However, the difficulty generally found in the determination of the mechanical properties of the vehicle, gave rise to proposals of simplified models where the motion of the car body and, sometimes, also the motion of the semi-sprung masses (bogies) are disregarded [10, 21]. A parametric study developed by the authors in order to discern the influence of the sprung and semi-sprung masses on the global dynamic response of the system, revealed that the vehicle model must comprise, at least, the dynamic behavior of the bogies and wheelsets [19].

3 EXPERIMENTAL ACTIVITIES

3.1 General description and objectives

In order to validate the numerical models developed by the authors, an experimental test site was selected and implemented in the Portuguese railway network (between Lisbon and Oporto), near to Carregado site.

Regarding the main aspects of the site, it must be referred that the track presents a straight alignment, corresponding to a renewed part of the railway connection between Porto and Lisbon. The line is composed by a double track on ballast, as illustrated in Figure 4, and distinct types of traffic are allowed in this line, ranging from freight trains up to passenger trains that circulate at speeds close to 220 km/h.



Figure 4 – General view of the site.

Two sets of experiments were performed: i) the first, to evaluate the dynamic properties of the track and of the ground; ii) the second, to measure the vibrations induced by the passage of the Alfa-Pendular train. Additionally, the track unevenness, key parameter for performing a dynamic train-track interaction analysis, was also measured.

The first set of experiments is used for the calibration of the numerical model and for a deeper understanding of the dynamic behavior of the track-ground system. On the other hand, the second set of experiments, comprising the response of the track-ground system during the passage of Alfa-Pendular train, is used for the experimental validation of the numerical model presented above.

3.2 Geodynamic characterization of the ground

Due to the uncertainty generally attributed to the ground properties, a detailed attention must be addressed to the geotechnical characterization of the ground. Following this logic three types of tests were performed in the site: i) one bore-hole with SPT tests spaced 1,50 m into depth; ii) two CPT tests; iii) two cross-hole tests.

Concerning the geotechnical scenario, the SPT and CPT tests allowed to find four main formations: i) up to 1.80 m to 2.00 m, the ground is mainly constituted by fine soil, overconsolidated; ii) between 1.80 m to 5.40 m, a relatively homogeneous formation is found, comprising clayey soils; iii) below 5.40 m and above 7.2 m, the ground is constituted by very soft organic layers intercalated with sand layers; iv) finally, for depths below 7.20 m, the ground is very homogeneous, corresponding to a thick layer of clays. Figure 5, shows the classification chart of the soil from the CPT tests, according the proposal of Robertson. The laboratorial tests confirmed this layering.

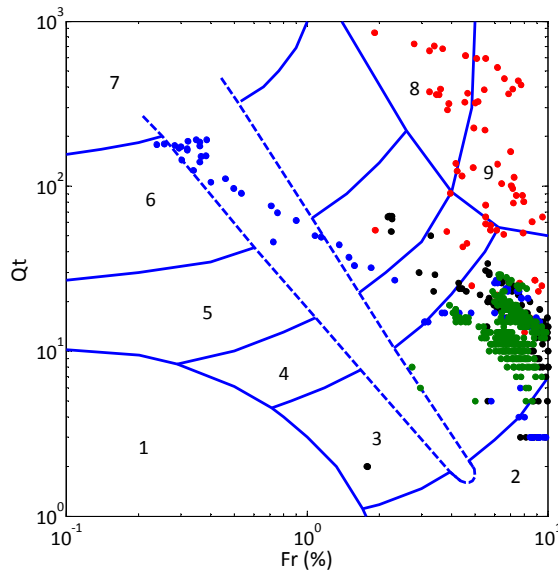


Figure 5 – Soil classification from the CPT test (red dots – $0\text{ m} < z < 1.8\text{ m}$; black dots – $1.8\text{ m} < z < 5.4\text{ m}$; blue dots – $5.4\text{ m} < z < 7.2\text{ m}$; green dots – $z > 7.2\text{ m}$).

The device used to perform the cross-hole tests enables to generate polarized S waves, allowing the measurement of P and S wave velocities. Figure 4 shows the measured wave velocities profile as well as the values adopted in the numerical model.

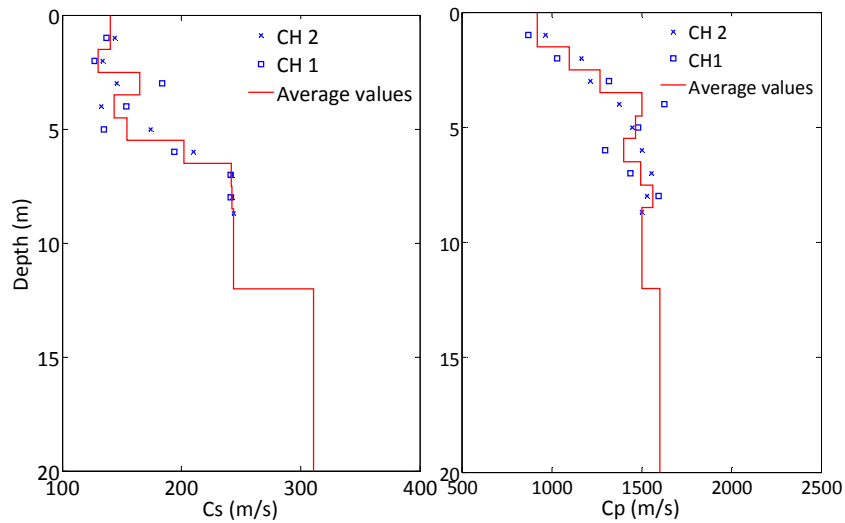


Figure 6 – Seismic wave velocities profile: a) Shear wave; b) Compressive wave.

A complete geodynamic characterization, for the purpose of the present study, should attend not only to the elastic properties of the ground but also to an estimation of the damping profile in depth.

In the present study, the damping profile was estimated from an inversion procedure based on the calibration of the numerical model in order to obtain a reasonable fit between measured and computed mobilities of the ground due to an excitation induced by a controlled source. The experimental setup adopted is shown on Figure 7.

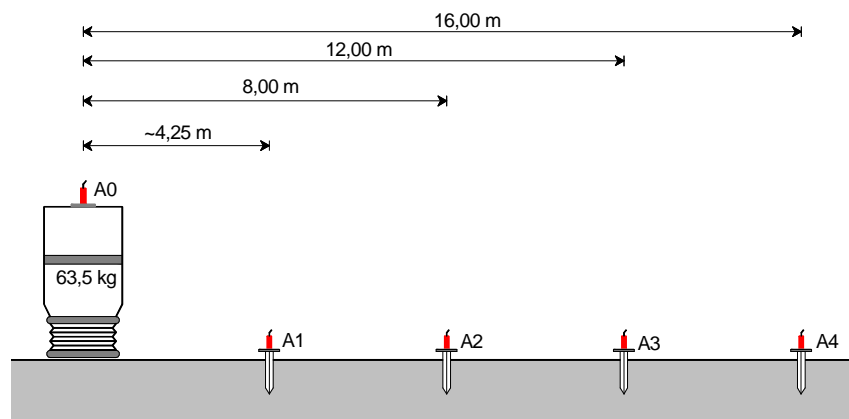


Figure 7 – Damping evaluation tests. Experimental setup.

From the acquired data, the experimental mobility is computed for the set of measuring points. On the other hand, a theoretical model was developed, taking into account the ground layering and stiffness properties described in Figure 6, where the damping profile is adjusted in order to obtain a reasonable fit between the measured and computed mobilities. Therefore, the only unknown variable in the numerical model is the damping of the ground, which gives rise to a simple inversion procedure. Figure 8 shows the modulus of the mobility measured and computed, for the 4 points of analysis. It is well patent in the figures that a reasonable fit between measured and computed results is achieved when the damping profile illustrated in Figure 9 is adopted.

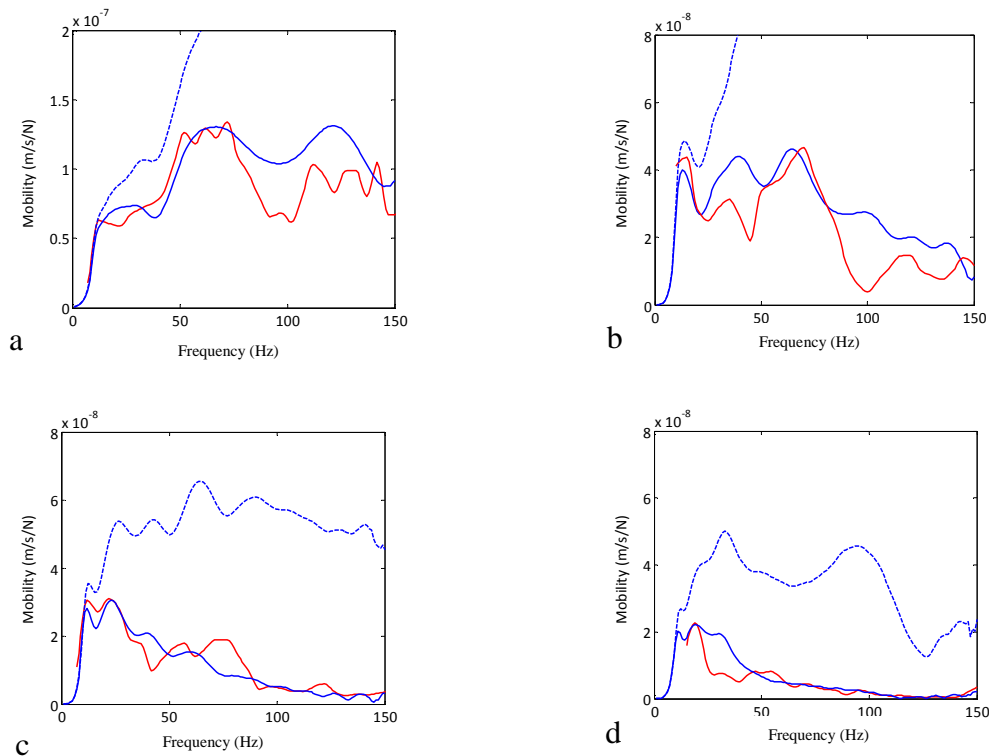


Figure 8 – Experimental and numerical mobility at different distances receiver-source:
a) 4.25 m; b) 8.00 m; c) 12.00 m; d) 16.00 m.

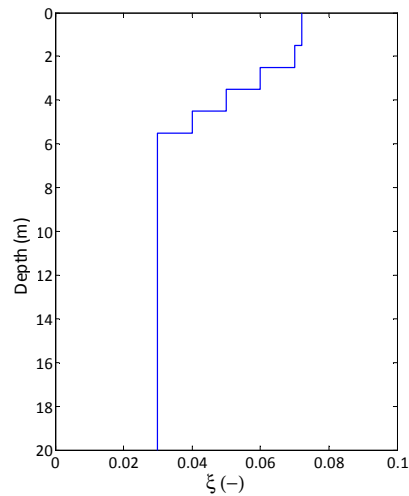


Figure 9 – Damping profile.

3.3 Assessment of the track mechanical properties

Another challenging usually found in the numerical analysis of railway tracks is due to the difficulty in the assessment of the properties of this complex structural system. If, by one hand, the properties of the rail and sleepers are well defined, the same statement cannot be extended to the other components such as the ballast or the railpads. In order to minimize the uncertainty related to properties of those elements, receptance tests were performed and the numerical model was calibrated, by an inversion procedure, in order to obtain a reasonable fit between the measured and computed receptances.

The adopted setup for the receptance tests is shown in Figure 10. As can be seen, the impact load (provided by an impulse hammer) is applied in the mid span of the sleeper and the response is measured by accelerometers installed on the sleeper extremities and on the rails.

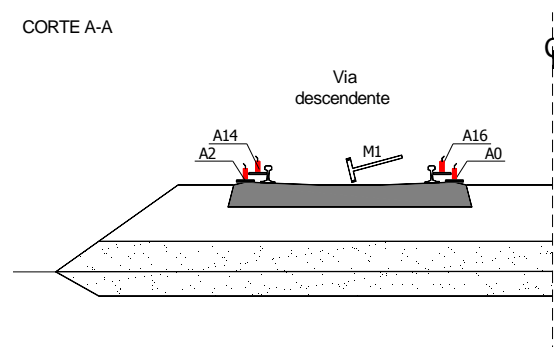


Figure 10 – Receptance tests setup.

A preliminary examination of the receptance of the rails enabled to confirm that very stiff railpads are used in this railway track. Through a simplified analysis it was found that the resonance frequency of the rails over the sleepers is related to a railpad stiffness of 700 kN/m, which is in correspondence with the value previously pointed out by the railpad manufacturer. Despite of the mentioned above, several variables (properties of the track elements) remain unknown, namely: the stiffness, the damping and the mass of the ballast and of subballast.

These properties are determined by the solution of a nonlinear least squares optimization problem with a residual that is a function of the track characteristics.

Figure 11 shows the geometry adopted for the numerical model, as well as the properties adopted after the optimization solution (see Figure 12). It should be noticed that the rail and sleepers were simulated according to the above mentioned properties of the materials. The layered ground was simulated by the 2.5D BEM procedure taking into account the stiffness, mass and damping provided by the set of tests described in the latter section.

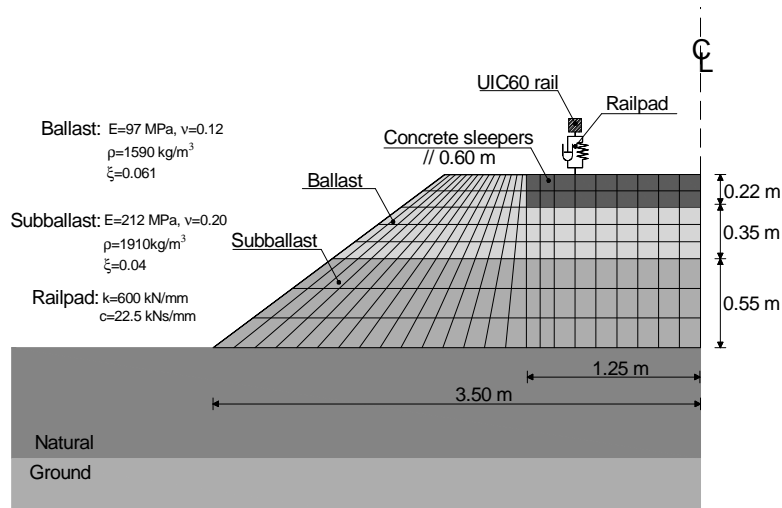


Figure 11 – Numerical model geometry and mechanical properties.

As is well patent is Figure 12, a reasonable agreement was found between measured and computed receptances, mainly for frequencies in the range between 70 Hz and 250 Hz.

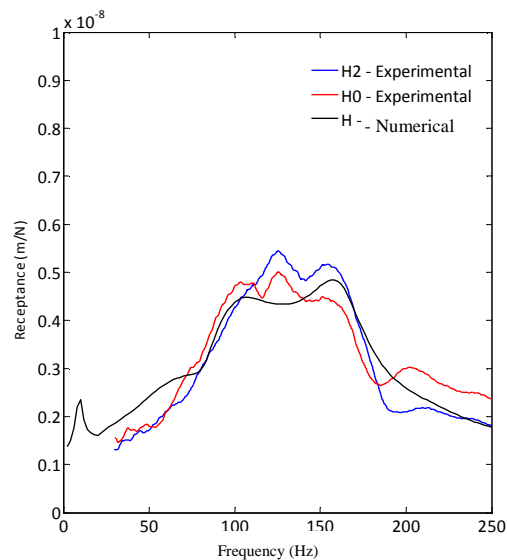


Figure 12 – Numerical and experimental sleeper receptance.

3.4 Measurement of track unevenness

As shown by equation 4, the knowledge of the track unevenness is a key parameter for the analysis of the dynamic excitation mechanism. Unlike other case studies, where the track un-

evenness is artificially generated, in the present study it was measured. Distinct equipments were used in order to have a reliable unevenness profile comprising the frequency bandwidth relevant to the analyses of vibrations induced by traffic. The recording car used by the Portuguese Railway Company (REFER) enables to measure the unevenness for wavelengths between 1.0 m and 25.0 m (Figure 13a). Therefore, for moderate running velocities, it is also necessary to know the short wavelength unevenness (also called rail corrugation) in order to take into account excitation frequencies up to 150 Hz. So, it was used a device that enabled the measurement of the wavelengths range between 0.4m and 1.0m. Both equipments are illustrated in Figure 13.



Figure 13 – Equipments for measuring the track unevenness: a) recording car; b) device for measuring the rail corrugation.

Figure 14 shows the measured unevenness profile of the right rail for the range of wavelengths between 0.4m and 25m. At a train speed of 212 km/h this range of wavelengths corresponds to an excitation frequency range of the vehicles between 2.1 Hz and 147 Hz. The reference section, i.e., the cross-section of the track and of the ground that was instrumented during the train passage, is also indicated in Figure 14.

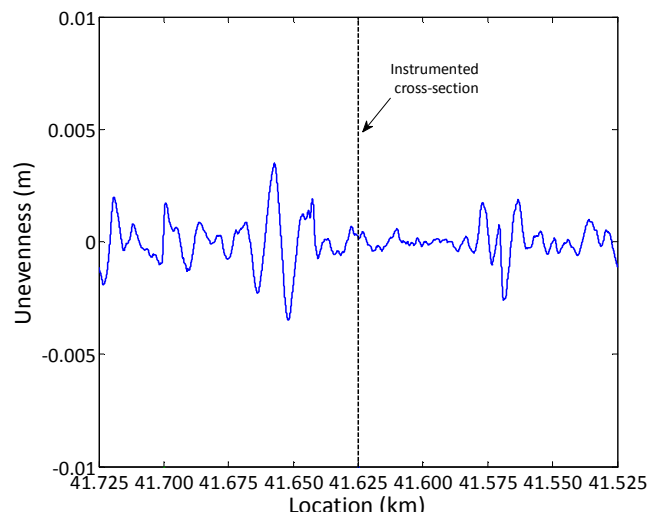


Figure 14 – Track unevenness profile.

3.5 Experimental assessment of vibrations induced by traffic

After the initial characterization experiments, focus was given to the measurement of track and free-field vibrations induced by traffic. Bearing this in mind, the setup illustrated in Figure 15 was implemented in order to experimentally evaluate the track-ground response due to traffic. As can be seen, the experimental setup comprised the measurement of vertical accelerations on the sleepers and on the ground surface, the latter at several distances from the track along a cross section. Complementarily, the displacement of the rail induced by the traffic was also measured by a laser device.

Although the huge amount of data acquired in this experimental test, subsequent to the passage of several distinct trains running at different speeds, in the following analysis only a fraction of the collected data was used, always regarding to the passage of the train Alfa-Pendular at a running speed of 212 km/h.

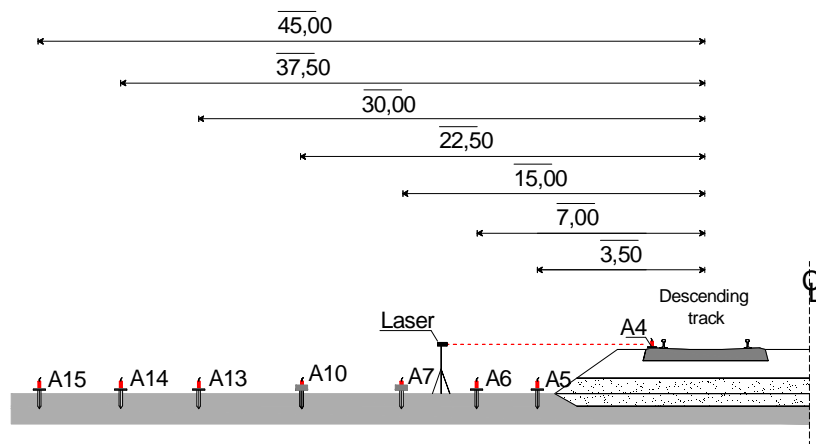


Figure 15 – Experimental setup.

4 EXPERIMENTAL VALIDATION

4.1 Model description

As emphasized before, the main objective of the study is the experimental validation of the numerical model presented in the initial sections of the paper. Thus, a numerical model comprising the train-track-ground dynamic interaction was constructed, in accordance to the formulation previously described.

The numerical model for the track-ground system is consistent with the information illustrated in Figure 11, reason why do not deserve more commentaries or justifications. Only a small remark must be done concerning to the difference between the real double-track geometry and the homologous adopted in the numerical modeling. In fact, as is well patent in Figure 11, the numerical model introduces a false plane of symmetry, crossing the mid span of the sleepers. An earlier sensibility study performed by the authors allowed concluding that this simplification is reasonable and doesn't give rise to an appreciable loss of accuracy in the prediction. Moreover, the numerical model was calibrated taking into account this "false" symmetry, reason why it is expected to obtain a good description of the physical reality through this model.

Concerning the rolling stock properties and the interaction mechanisms, in the following sections is considered the passage of train Alfa-Pendular at the speed of 212 km/h. The track

unevenness, in accordance to the results of the measurements presented in previous section, is included in the modeling procedure.

The Alfa-Pendular is the fastest train operating in Portugal. It is a conventional train composed by 6 vehicles, as indicated in Figure 16.

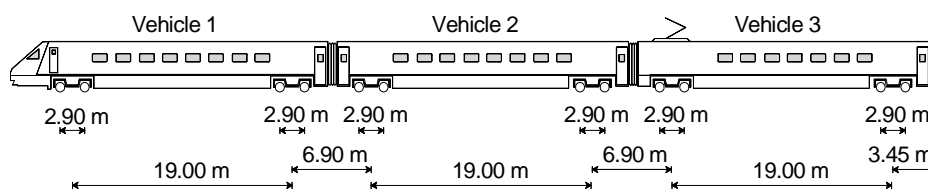


Figure 16 – Alfa Pendular geometry.

The main mechanical properties of the train were provided by the operator. In spite of this information, some identification modal tests for the structural characterization of the train were also developed and the properties adopted in the numerical model were adjusted in order to obtain a good fit between numerical and experimental natural frequencies. Table 1 summarizes the main properties of the train, in correspondence with the values adopted in the numerical analyses. The vehicles of the train are not exactly equal; Table 1 indicates the range of values found for the distinct vehicles of the train.

Table 1 – Train properties

Axles	Mw (kg)	1538-1884
Primary suspension	Kp (kN/m)	34200
	Cp (kNs/m)	36
Bogies	Mb (kg)	4712-4932
	Jb (kg/m ²)	5000-5150
Car body	Mc (kg)	32900-35710

A simplified structural model for the train was adopted. In that model, the motion of the sprung mass (car body) is discarded. However, this suffices for the purpose of the present study due to the fact that secondary suspension of the Alfa-Pendular train is soft enough to guarantee an efficient isolation of the car body for frequencies higher than few hertz.

4.2 The track dynamic response

Figure 17 compares the computed rail displacement with the measurement supplied by the laser device. In order to minimize the noise present in the measured signal, a low-pass filter with a cut-off frequency of 80 Hz was applied to both results.

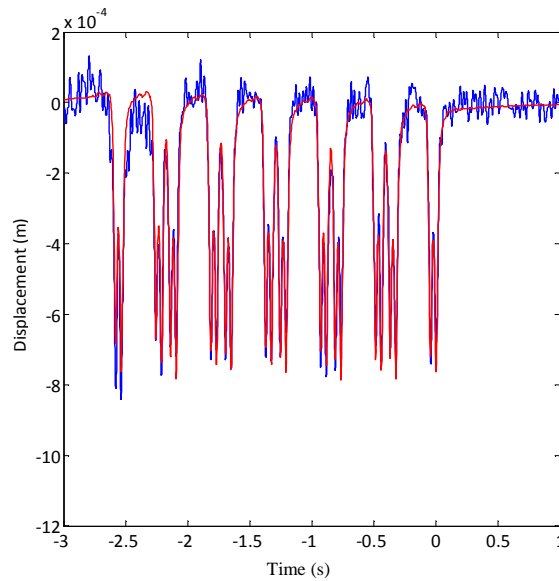


Figure 17 – Time record of the rail displacement (blue line – measurement; red line-computation).

As can be seen a splendid fit between rail displacement prediction and measurement was achieved. In fact, excluding a little discrepancy found during the passage of the first vehicle, the ability showed by the numerical model in the reproduction of the rail displacement is notorious.

Concerning the sleeper response, Figure 18 compares experimental and numerical time histories of the vertical velocity of the sleeper induced by the passage of the train Alfa-Pendular at 212 km/h.

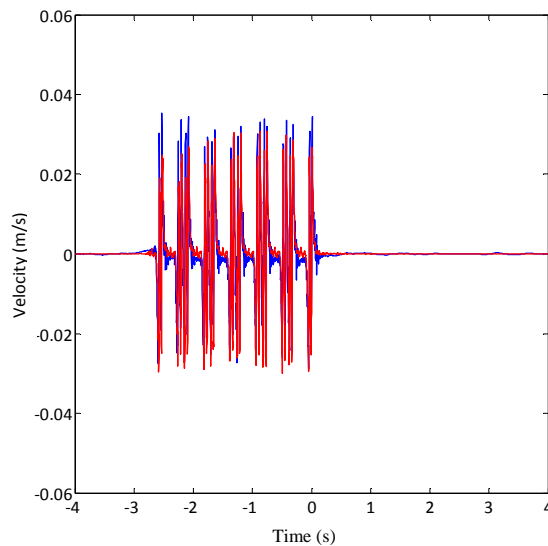


Figure 18 – Time record of the sleeper velocity (blue line – measurement; red line-computation).

Once again, a very good match between both results is emphasized by Figure 18. A clear distinction of the passage of each bogie is identified in the record, and a very good agreement between numerical and experimental results is found. Despite of the high quality of the results,

it must be noticed that slight differences between measurement and prediction are found for frequencies above 75 Hz.

4.3 The free-field dynamic response

Fulfilling the requirements of synthesis of this paper, only the results concerning the points of the ground closer to the track are here analyzed. The reader is invited to consult Alves Costa et al. [19] where complementary results are shown.

Figure 19 shows the time records of the vertical velocity of those points induced by the passage of train Alfa-Pendular at 212 km/h. The numerical prediction is overlapped to the experimental record.

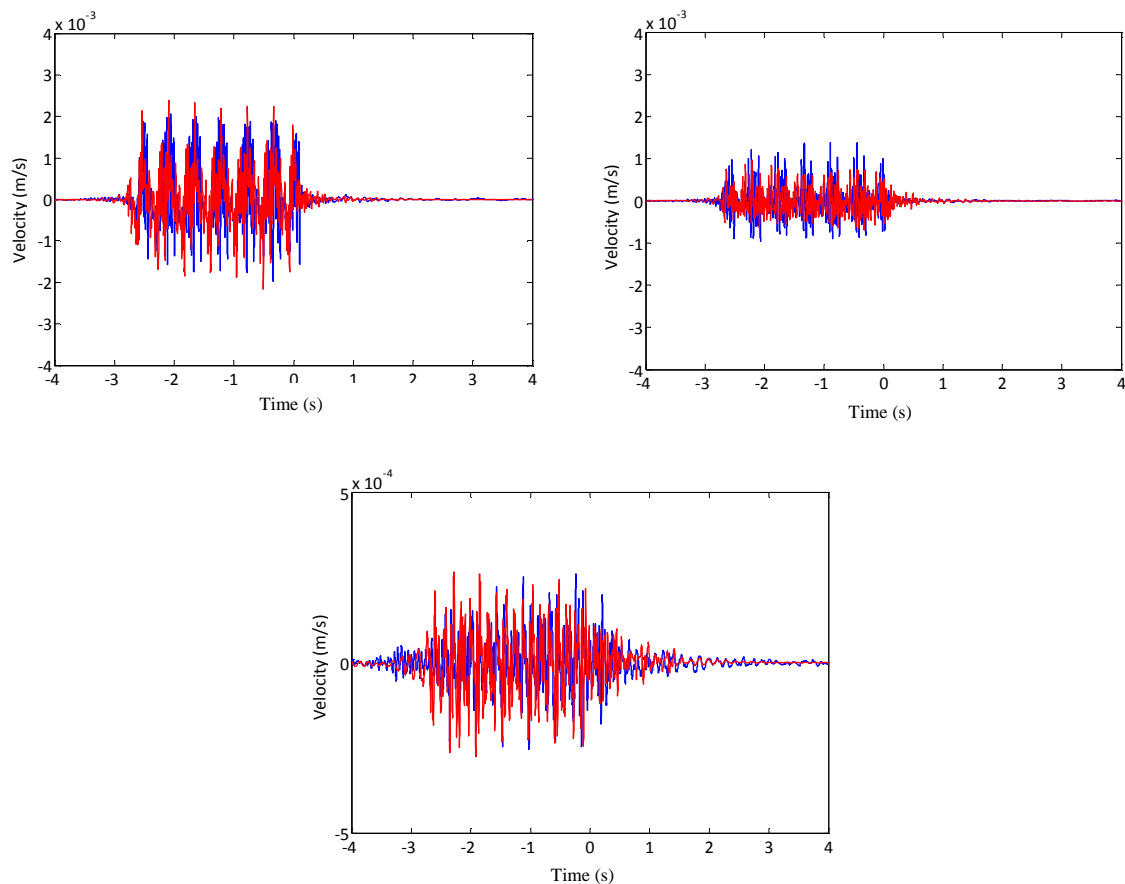


Figure 19 – Vertical velocity record at different distances from the track: a) 3.5 m; b) 7.0 m; c) 15.0 m (blue line – experimental; red line – computed).

Despite some differences between predicted and measured free-field vertical velocities, a reasonable agreement between simulation and physical reality was found. In fact, the numerical model was able to simulate the main aspects of the time record. However, a better discernment can be achieved by the analysis of the frequency content of the records, as illustrated in Figure 20.

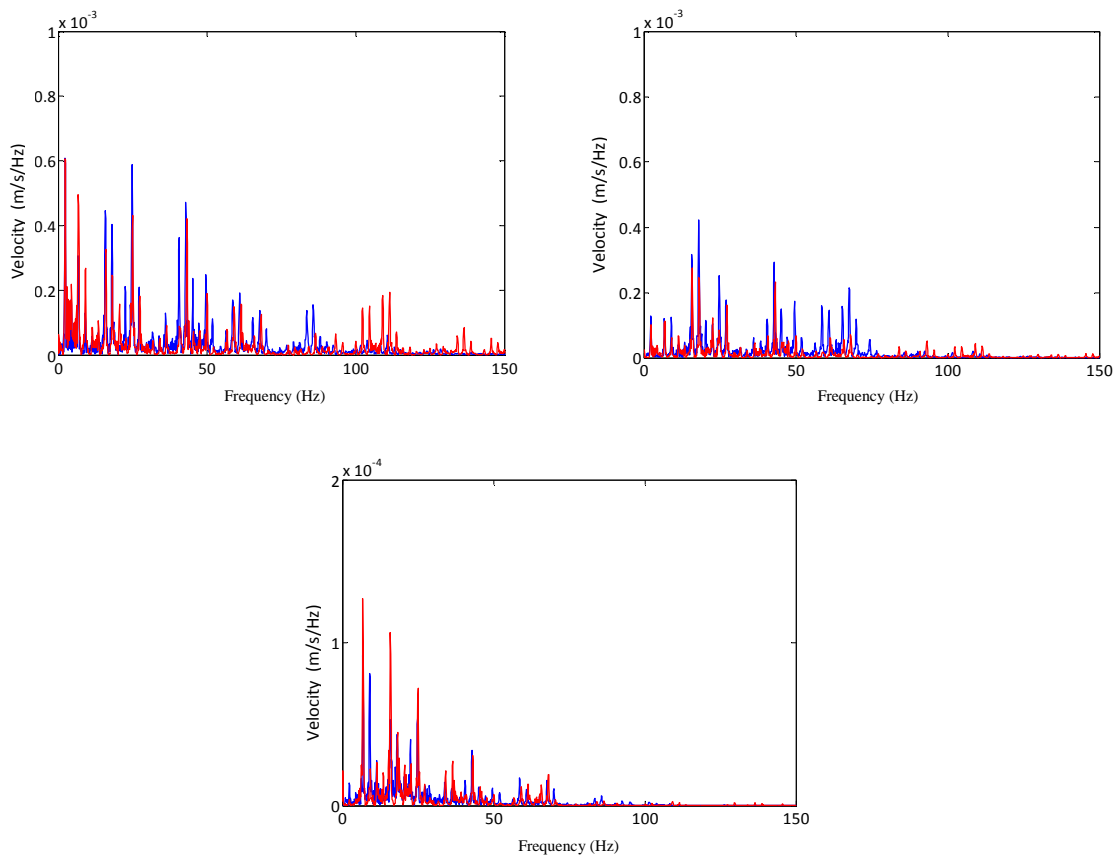


Figure 20 – Frequency content of the vertical velocity at different distances from the track: a) 3.5 m; b) 7.0 m; c) 15.0 m (blue line – experimental; red line – computed).

From the results exposed in Figure 20, one can conclude that the main characteristics of the frequency content were also well reproduced by the numerical model. Despite of this global good fit, for the point at a distance of 7.0 m, a more evident discrepancy between prediction and measurement is observed. Probably this difference is due to a local geotechnical condition of the ground that is distinct from the average scenario assumed in the simulation.

Despite of the successful obtained in the experimental validation of the model, it should be noticed that the discrepancy between prediction and measurement is much more evident when the analysis is focused on the dynamic response of the free-field than when the attention is dedicated to the track response. This fact shows well the complexity of the mechanisms of the wave propagation and the difficulty usually found in its numerical modeling.

5 CONCLUSIONS

In this paper, an experimental validation procedure of a 2.5D FEM-BEM model for the prediction of vibrations induced by railway traffic was shown.

The guidelines of the numerical model, implemented in Matlab 2009, were revealed, with special emphasis for the coupling procedure between the domains simulated by the 2.5 D FEM and the 2.5D BEM. Moreover, the model is able to perform train-track interaction analysis, aspect that was also described in the paper.

Bearing in mind the objective of the paper, an experimental test field, which was implemented in the Portuguese railway network, is described with emphasis to the experiments developed in order to calibrate the numerical model.

Finally, the vibrations measured during the passage of Alfa-Pendular train are compared with the prediction. The comparison between both results revealed a very good agreement for the track response and also for ground vibrations.

In the authors' opinion, the successful of this prediction is intrinsically related with a reliable characterization of the soil and of the track. Despite of the good fit reached between measurements and prediction, it should be noticed that the discrepancies between both results increases when the attention is focused on the prediction of free-field vibrations instead of track vibrations. This evidence is justified by the strong influence that local soil properties and inhomogenities of stiffness and damping can present on the waves propagation mechanisms.

ACKNOWLEDGMENTS

This paper reports research developed under the financial support of "FCT - Fundação para a Ciência e Tecnologia", Portugal, namely from the research project - PTDC/ECM/114505/2009. The first author wishes to thank FCT for the financial support provided by the grant SFRH / BD / 29747 / 2006.

The authors also wish to acknowledge the support of the project "Risk Assessment and Management for High-Speed Rail Systems" of the MIT – Portugal Program Transportation Systems Area.

The collaboration of REFER, CP and LNEC was also appreciated by the authors of the present work.

REFERENCES

1. Alves Costa, P., R. Calçada, A. Silva Cardoso, and A. Bodare, *Influence of soil non-linearity on the dynamic response of high-speed railway tracks*. Soil Dynamics and Earthquake Engineering, 2010. **30**(4): p. 221-235.
2. François, S., M. Schevenels, P. Galvín, G. Lombaert, and G. Degrande, *A 2.5D coupled FE–BE methodology for the dynamic interaction between longitudinally invariant structures and a layered halfspace*. Computer Methods in Applied Mechanics and Engineering, 2010. **199**(23-24): p. 1536-1548.
3. Dieterman, H.A. and A. Metrikine, *The equivalent stiffness of a half-space interacting with a beam. Critical velocities of a moving load along the beam*. European Journal of Mechanics A/Solids, 1996. **15**(1): p. 67-90.
4. Dieterman, H.A. and A. Metrikine, *Steady-state displacements of a beam on an elastic half-space due a uniformly moving constant load*. European Journal of Mechanics A/Solids, 1997. **16**(2): p. 295-306.
5. Sheng, X., C. Jones, and D. Thompson, *A comparison of a theoretical model for quasi-statically and dynamically induced environmental vibration from trains with measurements*. Journal of Sound and Vibration, 2003. **267**(3): p. 621-635.

6. Kausel, E., *Commentaries on methods to estimate ground vibrations elicited by fast moving loads*, in *Noise and Vibration on high-speed railways*, R.D. Calçada, R.; Carvalho, A., Degrande, G., Editor. 2008: Porto.
7. Yang, Y.B. and H.H. Hung, *A 2.5D finite/infinite element approach for modelling visco-elastic body subjected to moving loads*. International Journal for Numerical Methods in Engineering, 2001. **51**: p. 1317-1336.
8. Yang, Y., H. Hung, and D. Chang, *Train-induced wave propagation in layered soils using finite/infinite element simulation*. Soil Dynamics and Earthquake Engineering, 2003. **23**: p. 263-278.
9. Yang, Y. and H. Hung, *Soil Vibrations Caused by Underground Moving Trains*. Journal of Geotechnical and Geoenvironmental Engineering, 2008. **134**(11): p. 1633-1644.
10. Lombaert, G., G. DeGrande, J. Kogut, and S. François, *The experimental validation of a numerical model for the prediction of railway induced vibrations*. Journal of Sound and Vibration, 2006. **297**: p. 512-535.
11. Lombaert, G. and G. Degrande, *Ground-borne vibration due to static and dynamic axle loads of InterCity and high-speed trains*. Journal of Sound and Vibration, 2008. --(-----): p. -----.
12. Alves Costa, P., R. Calçada, J. Couto Marques, and A. Cardoso, *A 2.5D finite element model for simulation of unbounded domains under dynamic loading*, in *7th European Conference on Numerical Methods in Geotechnical Engineering*, T.B.a.S. Nordal, Editor. 2010: Trondheim. p. (aceite para publicação).
13. Galvín, P., S. François, M. Schevenels, E. Bongini, G. Degrande, and G. Lombaert, *A 2.5D coupled FE-BE model for the prediction of railway induced vibrations*. Soil Dynamics and Earthquake Engineering, 2010. **30**(12): p. 1500-1512.
14. Sheng, X., C. Jones, and D. Thompson, *Responses of infinite periodic structures to moving or stationary harmonic loads*. Journal of Sound and Vibration, 2005. **282**: p. 125-149.
15. Tadeu, A., J. Antonio, and L. Godinho, *Green's function for two-and-a-half dimensional elastodynamic problems in a half-space*. Computational Mechanics, 2001. **27**: p. 484-491.
16. Kausel, E., *An explicit solution for the green functions for dynamic loads in layered media*, R.R. R81-13, Editor. 1981, MIT: Boston.
17. Lopes, P., P. Alves Costa, R. Calçada, and A. Silva Cardoso, *Análise numérica de vibrações induzidas por tráfego ferroviário em túneis baseada em modelos 2.5D*, in *12º Congresso Nacional de Geotecnia*. 2010: Guimarães.
18. Sheng, X., C. Jones, and D. Thompson, *A theoretical study on the influence of the track on train-induced ground vibration*. Journal of Sound and Vibration, 2004. **272**: p. 909-936.
19. Alves Costa, P., R. Calçada, and A. Silva Cardoso, *Vibrations induced by railway traffic: influence of the mechanical properties of the train on the dynamic excitation mechanism*, in *EURODYN 2011*. 2011.
20. Zhai, W. and Z. Cai, *Dynamic Interaction between a lumped mass vehicle and a discretely supported continuous rail track*. Computers and Structures, 1997. **63**(5): p. 987-997.
21. Lombaert, G. and G. Degrande, *Ground-borne vibration due to static and dynamic axle loads of InterCity and high-speed trains*. Journal of Sound and Vibration, 2009. **319**(3-5): p. 1036-1066.